

## Structural, electronic, and optical properties of sphalerite ZnS compounds calculated using density functional theory (DFT)

A. M. Ghaleb\*, A. Q. Ahmed

*Department of Physics, College of Sciences, University of Kirkuk, Iraq*

This work studies the structure, electronic and optical properties of zinc blende ZnS by the use of the density functional theory (DFT) on the implemented in CASTEP code. In the generalized gradient approximation (GGA-PBESOL) and in the local density approximation (LDA) and, the exchange–correlation energy and band gap energies were measured. The estimated outcomes lattice constant, bulk modulus elastic constant agrees very well with the existing experiments and theories of data in structural optimization. Our calculated, direct band gap 2.23eV for LDA and 2.078eV for GGA, at the G point, agrees very well with the experiments. Also, we have measured the total (DOS) and partial (PDOS) densities of states. Furthermore, the absorption coefficient outcome is discussed in different incident phonon energies which was compared to the available experimental data.

(Received February 10, 2022; Accepted May 1, 2022)

*Keywords:* Castep code, DFT (LDA and GGA), Band gap, Optical properties

### 1. Introduction

Recently, the future II-VI semiconductor binaries and alloys in photonic, optoelectronic, and spintronic uses have attracted much attention[1-3]. Zinc sulfide (ZnS) is a significant semiconductor with outstanding chemical and physical features. It could benefit Optical coatings, solid-state solar window layers, electro optic modulators, photoconductors, field effect transistors, optical sensors, photo catalysts, and other light emitting materials. ZnS crystallizes in the hexagonal wurtzite (WZ) and face-centered cubic zinc blende (ZB) phases, according to reports. The band gap of ZnS is 3.50 eV for WZ structure and 3.82 eV for ZB structures[4]. Its defect-centered and self-activated luminescence's make ZnS emissions usually green and blue bands[5]. The capacity of ZnS to have a higher energy of exciton binding (40 MeV) than that of the thermal energy allows it to produce light at ambient temperature [6]. The lattice parameters for sphalerites (zinc blende) are  $a=b=c=5.4093\text{\AA}$ ,  $\alpha=\beta=\gamma=90^\circ$ , cell volume =  $158.279\text{\AA}^3$  as given in the experimental result of Skinner [7]. Sphalerites Zinc Sulphide (ZnS) has cubic structure with  $Z = 4$  and space group name  $F\bar{4}3m$  and space group number 216, sphalerite ZnS has a face centered cubic (FCC) lattice structure. Its atoms have the coordinates of  $T_d^2 - F\bar{4}3m$ [8]. The density-functional potential deficiencies for describing the semiconductors have been accused for the band gap theoretical underestimating of ZnS [9,10]. Besides getting the structural, electronic and optical properties, our obtained results are compared with Ref. [11]. Zakharov et al. utilized the pseudo potential methods and modified the d-characters in the valence band maximum (VBM) by the addition of a small value of attractive potentials in non-local d channel of the Zn pseudo potential for fitting the experimental positions[12]. The objective of this work is to study some properties of ZnS compound in preparation for knowing the possibility of using this compound, First, Study the electronic features of ZnS compound, then found a value for some electronic features including the energy band gap, lattice constant, elastic constant and optical properties such as absorption and comparing it with other experimental and theoretical results, in the next part we found and studied the entire and partial state densities in the characteristics that were studied before and also compared with the experimental and theoretical results.

\* Corresponding author: [abdlhadik@uokirkuk.edu.iq](mailto:abdlhadik@uokirkuk.edu.iq)  
<https://doi.org/10.15251/CL.2022.195.309>

## 2. Method of calculation

All measurements were conducted with the Cambridge serial total energy package (CASTEP) code. These measurements were performed according to the density functional theory (DFT) using the method of a plane-wave ultra-soft pseudo potential (USP) [13]. In a Kohn–Sham computation, the approximate functional used to determine exchange-correlation energy ( $E_{xc}$ ) has a significant impact on the correctness of the final findings. To get a rough estimate of  $E_{xc}$ , the exchange-correlation functional in the standard local density approximation (LDA) approach can be manipulated[14]. However the inhomogeneous electron densities in solids and the slow valence electron density fluctuations with space makes the use of the generalized gradient approximation (GGA) in the PBESOL scheme for computing electronic and optical characteristics a superior method to determining  $E_{xc}$ [15,16]. In this work using energy cutoff (350 eV), rounding was used LDA - CAPZ, to measure the correlation-exchange energy a pseudo potentials is used to explain the interactions of electrons with the nuclei of ions, we used ultra-soft. The grid parameters were  $6 \times 6 \times 6$  k-point set distributed uniformly in the Brillion region, and the relative treatment was Koelling-Harmon, The atomic calculation calculated for Zn and S are: (Zn:  $3s^2 3p^4$ ), (S:  $3d^{10} 4s^2$ ). And also used (394.6 eV) cutoff energy using GGA - PBESOL to treat the interaction of electrons with ions of the nuclei. And the correlation-exchange energy a pseudo potentials was OTEG ultra soft. The grid parameters were  $1 \times 1 \times 1$  k-point set in the Brillion region, The atomic calculation calculated in the program for Zn and S are (Zn:  $1s^2 2s^2 2p^6 3s^2 3p^6 3d^{10} 4s^2$ ), (S:  $1s^2 2s^2 2p^6 3s^2 3p^4$ ).

## 3. Result and discussion

### 3.1. Structural properties

Zinc sulphide (ZnS) is a group II-VI compounds that crystallizes in zinc blende (space group: 216/F43m). The atomic sites of Zn and S are (0, 0, 0) and (1/4, 1/4, 1/4) in the primitive unit cells respectively. Figure 1 shows the crystal symmetries of the compounds under study and their computed structural parameters. However, the results from the literature experiments literature and those of our study are in Table 1. The equilibrium lattice constant results, the bulk modulus, and its pressure derivative are calculated by fitting the outcome data of the equilibrium energy and volume to the 2<sup>nd</sup> order Murnaghan's equation of state(EOS) [17]. The obtained outcomes reveal that our calculations are reasonable.

$$E(V) = E_0 + \frac{B_0 V}{\dot{B}_0} \left[ \frac{\left(\frac{V_0}{V}\right)^{\dot{B}_0}}{B_0 - 1} + 1 \right] - \frac{B_0 V_0}{B_0 - 1} \quad (1)$$

In the above equations,  $B_0$  is the volumetric modulus,  $\dot{B}_0$  is its first derivative in terms of pressure,  $V_0$  stands the equilibrium volume at 0 temperature, and  $E_0$  is the structure's equilibrium energy. After the investigation of structural properties of ZnS are found in good agreement with the experimental data. This indicates that the use of approximations (LDA and GGA) in structural calculations was good, except for a very small difference in bulk modules and volumes.

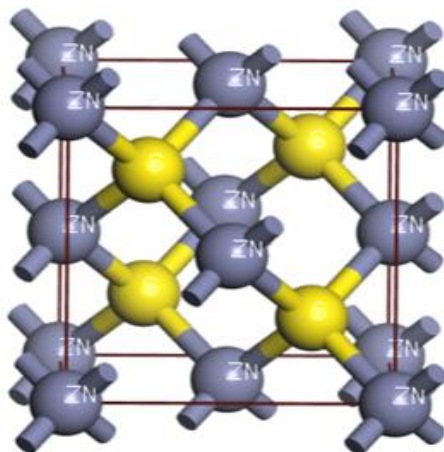


Fig. 1. Zinc-blende ZnS compound crystal structure.

Table 1. Values of lattice constant, bulk modulus and cell volume for ZnS.

Compound		present work		Experimental work		Other theoretical work	
		LDA	GGA	[18]	[19]	[20]	[21]
ZnS	$a$ (Å)	5.3	5.4	5.41	5.41	5.33	5.44
	$B$ (GPa)	93.8	61.6	75.00	76.9	83.16	81.30
	$V$ (Å <sup>3</sup> )	148	162	154.05[22]		161.99[1]	

### 3.2. Elastic constants

The ZnS three free elastic constants are  $C_{11}$ ,  $C_{12}$  and  $C_{44}$  defining the mechanical the material stability. They are often inferred by measuring the total energy which represents the elastic features of the crystal. We can get any stability condition of the cubic crystal through: (2).

$$C_{11} - C_{12} > 0, C_{11} + 2C_{12} > 0, C_{44} > 0 \quad (2)$$

$C_{11} > |C_{12}|$  are the first condition while the first and second indicate that  $C_{11} > 0$ . The elastic constant values measured with the LDA and the GGA (Table 1) meet these conditions of stability. Thus, the zinc blende ZnS structure is stable mechanically. In the analysis of the findings which are obtained by the two approximations, we can see the sequence  $C_{11} > C_{12} > C_{44}$ , which agree with those got from the experiment [20] and theory [23] in Table 2. Yet, the LDA (GGA) overestimates (underestimates) the experiment values of  $C_{11}$  and  $C_{12}$  ( $C_{11}$ ,  $C_{12}$  and  $C_{44}$ ), and there is an underestimation of  $C_{44}$  value. The elastic constant results show that the anisotropy coefficient  $A$  of the ZnS was obtained by the relation (3) [24], representing a calculation of the crystal anisotropy. The material of a perfectly isotropic has  $A$  with a value of 1, thus, values lower or higher than the unity could be the value of the crystal anisotropy. The measured  $A$  values were 0.44 for the LDA and 0.39 for the GGA. So, ZnS is a perfect isotropic in terms of elasticity confirming [20] and [23]. These authors state that  $A$  is a pressure free and equal 0.5 in the ZnS zinc-blende phase.

$$A = \frac{C_{11} - C_{12}}{2C_{44}} \quad (3)$$

Table 2. Elastic constant calculated through CASTEP, in GPa units, compared to experimental data and other theoretical calculations.

ZnS		$C_{11}$	$C_{12}$	$C_{44}$
Present work	(LDA)	115.9	69.52	52.69
	(GGA)	104.4	61.63	54.79
Other Cal.[20]		108.83	69.18	45.50
Exp.[23]		104	65	46.2

### 3.3. Electronic band structures and density of state

Now energy band is used with the Brillouin zone high-symmetry points by LDA and GGA as in Fig.2, discuss the results of the electronic properties of zb-ZnS. A direct band gap at G point for zb-ZnS is 2.232eV eV in LDA result (2.078 eV in GGA). Yet, the direct energy band gap at ( $\Gamma - \Gamma$ ) is point in [25,26]. Because the band gap value ranges are (G – G) and ( $\Gamma - \Gamma$ ), they are very close. Furthermore, the methods of a plane-wave basis set and pseudo potentials in present calculation is employed, calculations are conducted by the full potential linearized augmented plane wave (FP-LAPW) method used WIEN2K code [25,26]. So, the energy gap differs from that in [26,27]The LDA measured band gap confirms past theoretical values (2.83eV) [25,26] although they smaller those of the experiment value 3.5 eV [27] because of the famous underestimating conduction band state energies in calculating the DFT. The Fermi level is the energy in which the probability is half of the used state. For chemical potential states ( $\mu$ ) = Fermi level ( $E_F$ ), the Fermi distribution function  $f(\mu) = 1/2$ . i.e. half of the states with  $\mu = E_F$  are employed. The energy scale zero is set at the valence band(VB) top. We calculated the energy band structures with the directions with high first brillouin zone equilibrium points, including X→R→M→G→R. A direct energy inhibitor appears between the highest valence band value and the lowest conduction band value at the symmetry point G of the brillion region of the compound ZnS. Table 3 shows all the direct band gaps in comparison with those experiments[27] and theories [25,26].Table 3 is the band gap in LDA which is higher than that in GGA. Possibly, it is because of the lower lattice constants estimated LDA and the alteration in methods of GGA and LDA dealing with the electron density.

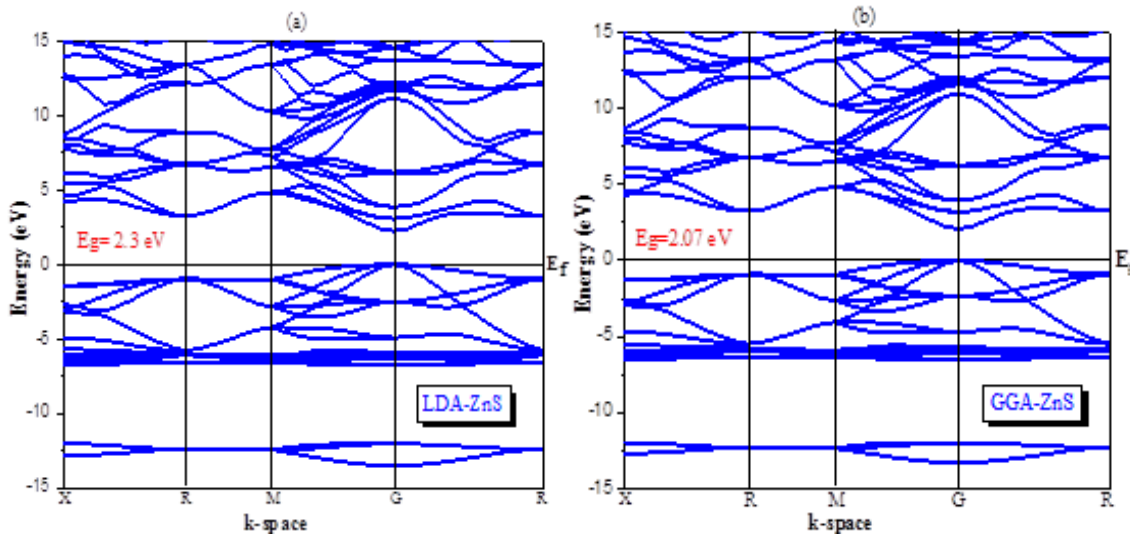


Fig. 2. Electronic band gap structure of zb-ZnS applying (a)LDA, (b)GGA approximation.

Table 3. Calculated energy gap in eV of zb-ZnS with available theoretical and experimental values.

Methods			
LDA (present work)	GGA (present work)	Other Cal.	Exp.
2.232	2.078	1.87 <sup>a</sup> , 2.03 <sup>b</sup>	3.5 <sup>c</sup>

<sup>a</sup>Ref.[25], <sup>b</sup> Ref.[26], <sup>c</sup> Ref.[27].

The total DOS outcomes in Fig 3(a and b). indicates band gap separates the valence and conduction bands of ZnS. The gap is measured by LDA and GGA. In the ZnS zinc-blende structure, the state valence band densities could be classified into three regions. Here, the valence band maximum as the Fermi level use could make the region about -5 eV occupied by p-states from S atoms, where there is a small influence of Zn s-states. They are a near -6 eV to -7.5 eV could be mainly Zn d-states, with a small impact of S p-states. This structure resembles the flat bands in the ZnS electronic band structures as in Fig 2(a,b). The total DOS is much lower than the valence band, at around -13.5eV, coming dominantly from the S s-states and also matching the lowest valence band in the measured ZnS band structure. The general TDOS profiles agree with the past theoretical calculations [25]. Besides, it is inferable from that the absorption onset very sharp starting at 3.73 eV. Sharp peaks emerged at 4.86 eV, 6.7 eV and 8.6 eV in the low laying conduction bands. In terms of the valence bands DOS, peaks at -13.80 eV, -6.56 eV, -5.1 eV, -3.5 eV, -2.99 eV and -1.99 eV are calculated and seem similar approximately to those of the corresponding experimental, from x-ray spectroscopy [28].

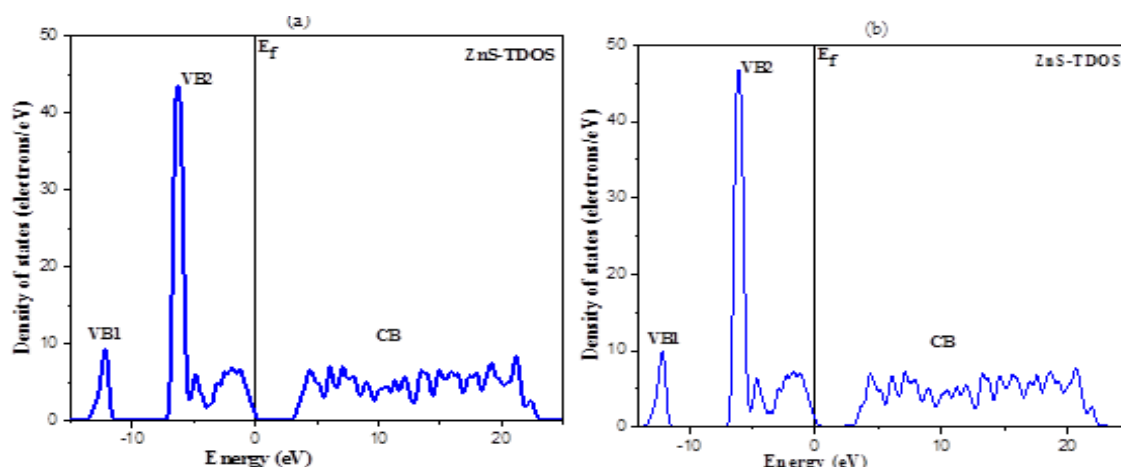


Fig. 3. The total density of states (TDOS) for ZnS (a)LDA, (b)GGA.

Fig 4(a and b). Show PDOS for zb-ZnS calculation using LDA and GGA where as the green, red and blue indicate ( d , p and s) states .Generally, the valence band has three main regions : the deep originating from S-2s state, the middle derived from Zn-3d state and partially from S-2p state, and the shallow originating from S-2p state. The conduction is controlled by the Zn-4s and S-2p state. The valance band primarily controlled by the d-state (Zn atom) with an increasing contribution according to orders of LDA > GGA. The intensity rise in the GGA calculation improves treating the band structure better than the LDA method.

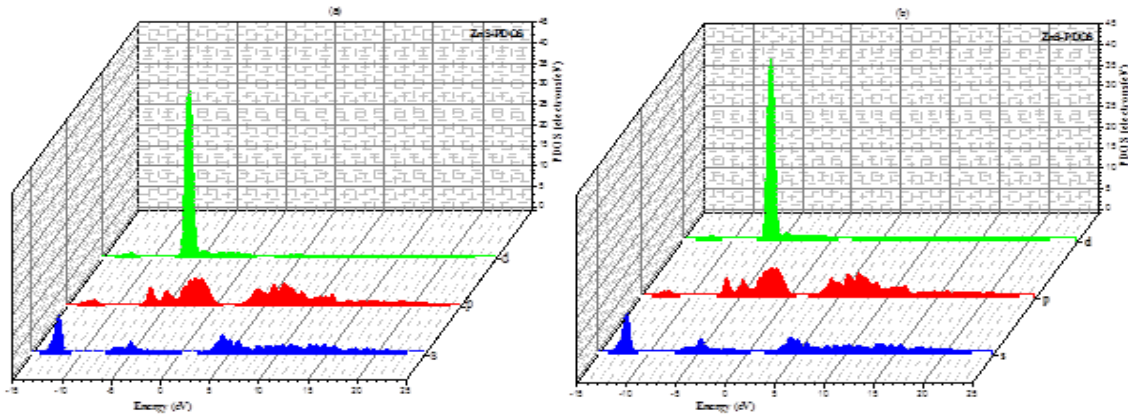


Fig. 4. The partial density of states (PDOS) for ZnS (a)LDA, (b)GGA.

### 3.4. Optical properties

The optical properties are utilized for studying the interactions between incident photons and ZnS solid solutions assisting in the establishment of the photo catalytic reactor with radiation field spatial distribution. Also the knowledge of solid optical properties assists to understand its electronic features. When a photon is absorbed by an object, it induces an electrical leap from an occupied state in the valence band to an empty state in the conduction band, Fig 5 (a and b) shows the optical absorption coefficient spectrum of the compound studied. This properties investigations were done within the chosen energy range of (0- 35) eV using both DFT(LDA) and DFT(GGA) whereas absorption spectra define materials ability to harvest or trap electromagnetic radiation or incident light, absorption value of  $(3.1E5) \text{ cm}^{-1}$  and  $(2.9E5) \text{ cm}^{-1}$  were measured at optical peaks of (8 eV) and (8.5eV) for LDA and GGA respectively. GGA calculated absorption showed higher capability of light absorption compared to LDA approximation and this results good agreement with experimental value absorption value of  $(9.97E5) \text{ cm}^{-1}$  and optical peaks (6.8eV) [29]. The absorption spectrum shows a peak in a low energy value while the strong optical absorption peaks are mainly in regions of high energy (6 - 10 eV), corresponding to the transitions of the inter bands. In contrast, there is positive correlation between absorption decreases and energy of the photon within a high-energy ranges higher than the 10 eV), in which the electron has a hard response. Therefore, the electrons in the VB can be excited to the CB by absorbing visible light. The optical absorption of ZnS in the UV light region occurs by electron transfer from the  $S_{2p}$  orbital of valence band to the  $Zn_{3s}$  orbital of conduction band [30].

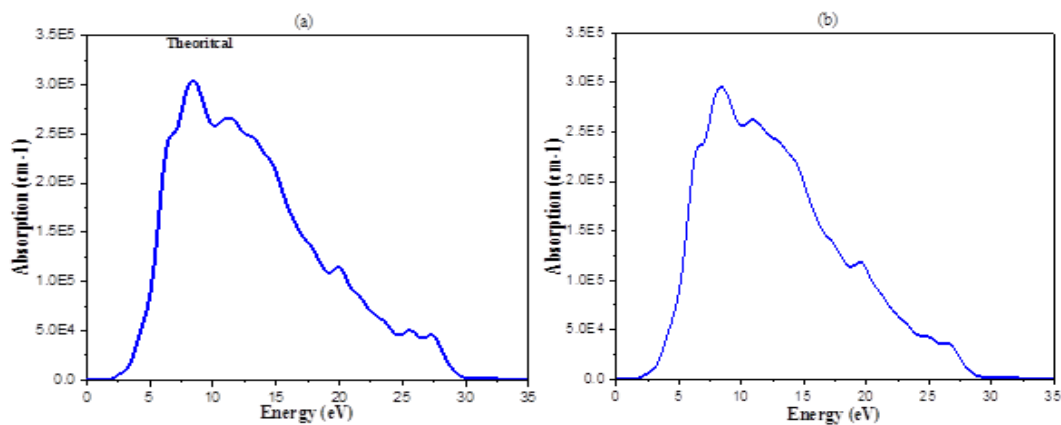


Fig. 5. Absorption coefficient for ZnS in (a)LDA, (b)GGA approximations.

### 3.5. Charge density distribution

Using the LDA To study the bonding nature between the atoms of ZnS , the valence electron charge density distributions ( $e/A^3$ ) within the (3D) and (110) planes are depicted in Fig 6. The color scale between the maps represents the local electron density. Red and blue colors indicate lowest and highest electron density, respectively. The above maps of charge density distributions show that the charge distribution is around the S atomic species and is considerably distorted of spherical shape because of the surrounding Zn atom charge distribution. This is an indication of covalent bonding. Since charge on S atoms is higher than those of the Zn atoms, there is also ionic contribution. In the charge density distribution maps. There are obvious signatures of covalent bonding Zn-Zn, Zn-S and S-S atoms ZnS compounds. These findings confirm the Mullikan bond population analyses (“Bond population analysis” section) For 3D and plane (110). The ZnS charge density maps show that Zn atom possesses high electron densities in comparison with S atom. Zn and S atoms are electron deficient in ZnS with spherical charge distributions. These characteristics entails ionic contributions to the whole bonding.

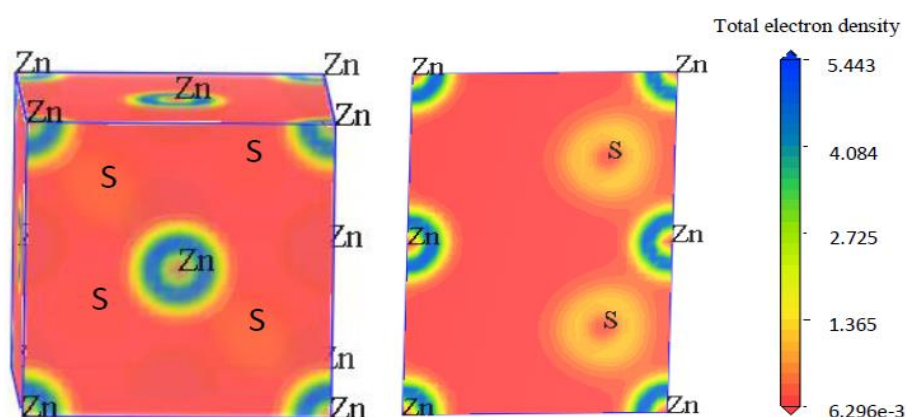


Fig. 6. Charge density distribution map of ZnS (a) (3D) and (b) (110) planes using LDA.

### 3.6. Bond population analysis

Both Mulliken population analysis (MPA) [31] were used to explore the bonding nature of ZnS compound further. The results are disclosed in Tables 4 and 5. According to MPA, in ZnS the Zn atom gives up 0.4 charge to each S atom. As usual, Mulliken charge and overlap population is to evaluate the chemical bond relative strength among the atoms. Also, we utilized the effective valence [32] for determining the covalent or ionic bonding dominance. This valence is a perfect ionic bond which is 0, while the corresponding is higher than this ionic bond if the bond becomes covalent. Table 4 shows the whole and the effective valence charges of Zn and S species ZnS. The charges transferring from S and Zn are about (-0.4e, 0.4e in LDA) and (-0.45e and 0.45e in GGA). Thus, the bonding behavior of ZnS coexists with the natures of covalent and ionic. Table 5 shows the measured outcomes of the Mulliken bond populations and bond lengths in ZnS through the use of functions of LDA and GGA. The negative and positive bond population values are the antibonding and bonding states in respect. The Mulliken bond population of the Zn-S (LDA) is  $2.35481A^0$  ( $2.40466$  with GGA) which is the value LDA as smaller than the GGA. These findings confirm the analyses of the electronic structures and densities of the states mentioned above.

Table 4. Orbital charges (electron), Total charge and atomic Mulliken charge (electron) of ZnS using LDA and GGA.

Methods	Species	s	p	d	f	Total	Mulliken Charge (e)
LDA	S	1.81	4.59	0.00	0.00	6.40	-0.40
	Zn	0.61	1.02	9.97	0.00	11.60	0.40
GGA	S	1.83	4.63	0.00	0.00	6.45	-0.45
	Zn	0.59	0.98	9.98	0.00	11.55	0.45

Table 5. Calculated bond overlap populations and bond lengths ( $\text{\AA}$ ) for ZnS using LDA and GGA.

Methods	Bond	Population	Length (A)
LDA	Zn -- S	0.46	2.35481
GGA	Zn -- S	0.44	2.40466

#### 4. Conclusions

We have investigated the energy band structure, elastic constants, density of states, optical properties, and bonding properties of Zb-ZnS using first principles calculations. The equilibrium lattice parameters, bulk modulus and its pressure derivative of Zb-ZnS are optimized, and the calculated results by LDA and GGA are consistent with the experimental data and the available theoretical results. The elastic constants are firstly predicted by the methods of LDA and GGA. Our calculations reveal that Zb-ZnS shows elastic anisotropy and elastic stability under ambient conditions. Our results for the band structures and DOS show that Zb-ZnS is semiconductor with a direct band gap. The energy band gap is estimated to be 2.232eV (LDA) or 2.078eV (GGA), which are both underestimated and compared with the experimental band gap. Based on the calculations of the density of states and Mulliken population, the chemical bonding indicated both ionic and covalent bonding in Zb-ZnS. Our calculated optical absorption is in a good agreement with the obtained experimental results.

## References

- [1] Karazhanov, S. Z., Ravindran, P., Kjekshus, A., Fjellvåg, H., & Svensson, B. G. (2007). Electronic structure and optical properties of Zn X (X= O, S, Se, Te): A density functional study. *Physical Review B*, 75(15), 155104; <https://doi.org/10.1103/PhysRevB.75.155104>
- [2] Nurmikko, A., & Gunshor, R. L. (1997). Blue and green semiconductor lasers: a status report. *Semiconductor science and technology*, 12(11), 1337; <https://doi.org/10.1088/0268-1242/12/11/003>
- [3] Zehnder, U., Yakovlev, D. R., Ossau, W., Gerhard, T., Fischer, F., Lugauer, H. J., ...& Landwehr, G. (1998). Optical properties of laser diodes and heterostructures based on beryllium chalcogenides. *Journal of crystal growth*, 184, 541-544; [https://doi.org/10.1016/S0022-0248\(97\)00704-5](https://doi.org/10.1016/S0022-0248(97)00704-5)
- [4] Long, D., Li, M., Meng, D., & He, Y. (2018). Electronic-structure and thermodynamic properties of ZnS<sub>1-x</sub>Se<sub>x</sub> ternary alloys from the first-principles calculations. *Computational Materials Science*, 149, 386-396; <https://doi.org/10.1016/j.commatsci.2018.03.046>
- [5] Morozova, N. K., Karetnikov, I. A., Plotnichenko, V. G., Gavrishchuk, E. M., Yashina, E. V., & Ikonnikov, V. B. (2004). Transformation of luminescence centers in CVD ZnS films subjected to a high hydrostatic pressure. *Semiconductors*, 38(1), 36-41; <https://doi.org/10.1134/1.1641130>
- [6] Sun, C. W., Jeong, J. S., & Lee, J. (2006). Microstructural analysis of ZnO/ZnS nanocables through Moiré fringe induced by overlapped area of ZnO and ZnS. *Journal of crystal growth*, 294(2), 162-167; <https://doi.org/10.1016/j.jcrysgro.2006.06.023>
- [7] Skinner, B. J. (1961). Unit-cell edges of natural and synthetic sphalerites. *American Mineralogist: Journal of Earth and Planetary Materials*, 46(11-12), 1399-1411.
- [8] Tilley, R. J. (2020). *Crystals and crystal structures*. John Wiley & Sons.
- [9] Perdew, J. P., & Levy, M. (1983). Physical content of the exact Kohn-Sham orbital energies: band gaps and derivative discontinuities. *Physical Review Letters*, 51(20), 1884; <https://doi.org/10.1103/PhysRevLett.51.1884>
- [10] Karazhanov, S. Z., & Voon, L. L. Y. (2005). Ab initio studies of the band parameters of III-V and II-VI zinc-blende semiconductors. *Semiconductors*, 39(2), 161-173; <https://doi.org/10.1134/1.1864192>
- [11] Imai, Y., Watanabe, A., & Shimono, I. (2003). Comparison of electronic structures of doped ZnS and ZnO calculated by a first-principle pseudopotential method. *Journal of Materials Science: Materials in Electronics*, 14(3), 149-156.
- [12] Zakharov, O., Rubio, A., Blase, X., Cohen, M. L., & Louie, S. G. (1994). Quasiparticle band structures of six II-VI compounds: ZnS, ZnSe, ZnTe, CdS, CdSe, and CdTe. *Physical Review B*, 50(15), 10780; <https://doi.org/10.1103/PhysRevB.50.10780>
- [13] Clark, S. J., Segall, M. D., Pickard, C. J., Hasnip, P. J., Probert, M. I., Refson, K., & Payne, M. C. (2005). First principles methods using CASTEP. *Zeitschrift für Kristallographie-Crystalline Materials*, 220(5-6), 567-570; <https://doi.org/10.1524/zkri.220.5.567.65075>
- [14] Kohn, W., & Sham, L. J. (1965). Self-consistent equations including exchange and correlation effects. *Physical review*, 140(4A), A1133; <https://doi.org/10.1103/PhysRev.140.A1133>
- [15] Perdew, J. P. (1996). S Burke and M Ernzerhof *Phys. Rev. Lett.*, 77, 3865; <https://doi.org/10.1103/PhysRevLett.77.3865>
- [16] Juan, Y. M., Kaxiras, E., & Gordon, R. G. (1995). Use of the generalized gradient approximation in pseudo potential calculations of solids. *Physical Review B*, 51(15), 9521; <https://doi.org/10.1103/PhysRevB.51.9521>
- [17] Murnaghan, F. D. (1944). The compressibility of media under extreme pressures. *Proceedings of the national academy of sciences of the United States of America*, 30(9), 244; <https://doi.org/10.1073/pnas.30.9.244>
- [18] Ves, S., Schwarz, U., Christensen, N. E., Syassen, K., & Cardona, M. (1990). Cubic ZnS under pressure: Optical-absorption edge, phase transition, and calculated equation of state. *Physical Review B*, 42(14), 9113; <https://doi.org/10.1103/PhysRevB.42.9113>

- [19] Strehlow, W. H., & Cook, E. L. (1973). Compilation of energy band gaps in elemental and binary compound semiconductors and insulators. *Journal of Physical and Chemical Reference Data*, 2(1), 163-200; <https://doi.org/10.1063/1.3253115>
- [20] Ferahtia, S., Saib, S., & Bouarissa, N. (2019). Computational studies of mono-chalcogenides ZnS and ZnSe at high-pressures. *Results in Physics*, 15, 102626; <https://doi.org/10.1016/j.rinp.2019.102626>
- [21] Ullah, N., Ullah, H., Murtaza, G., Khenata, R., & Ali, S. (2015). Structural phase transition and optoelectronic properties of ZnS under pressure. *J. Opt. Adv. Mater*, 17, 1272.
- [22] Soltani, N., Dehzangi, A., Kharazmi, A., Saion, E., Yunus, W. M. M., Majlis, B. Y., ...&Khalilzadeh, N. (2014). Structural, optical and electrical properties of ZnS nanoparticles affecting by organic coating. *Chalcogenide Letters*, 11(2), 79-90.
- [23] Berlincourt, D., Jaffe, H., & Shiozawa, L. R. (1963). Electroelastic properties of the sulfides, selenides, and tellurides of zinc and cadmium. *Physical Review*, 129(3), 1009; <https://doi.org/10.1103/PhysRev.129.1009>
- [24] Sadao, A. (2005). *Properties of group-iv, iii-v and ii-vi semiconductors*. Hoboken (USA) Wiley&Sons.
- [25] Noor, N. A., Ikram, N., Ali, S., Nazir, S., Alay-e-Abbas, S. M., & Shaukat, A. (2010). First-principles calculations of structural, electronic and optical properties of  $Cd_xZn_{1-x}S$  alloys. *Journal of Alloys and Compounds*, 507(2), 356-363; <https://doi.org/10.1016/j.jallcom.2010.07.197>
- [26] Rashid, M., Noor, N. A., Sabir, B., Ali, S., Sajjad, M., Hussain, F., ...&Khenata, R. (2014). Ab-initio study of fundamental properties of ternary  $ZnO_{1-x}S_x$  alloys by using special quasi-random structures. *Computational materials science*, 91, 285-291; <https://doi.org/10.1016/j.commatsci.2014.04.032>
- [27] Kumar, P., Misra, A., Kumar, D., Dhama, N., Sharma, T. P., & Dixit, P. N. (2004). Structural and optical properties of vacuum evaporated  $Cd_xZn_{1-x}S$  thin films. *Optical Materials*, 27(2), 261-264; <https://doi.org/10.1016/j.optmat.2004.04.008>
- [28] Ley, L., Pollak, R. A., McFeely, F. R., Kowalczyk, S. P., & Shirley, D. A. (1974). Total valence-band densities of states of III-V and II-VI compounds from x-ray photoemission spectroscopy. *Physical Review B*, 9(2), 600; <https://doi.org/10.1103/PhysRevB.9.600>
- [29] Adachi, S. (2013). *Optical constants of crystalline and amorphous semiconductors: numerical data and graphical information*. Springer Science & Business Media.
- [30] Ghaleb, A.M., Munef, R.A., Mohammed, S.F.( 2022). First principles study the effect of Zn doped MgO on the energy band gap using GGA approximation. *Journal of Ovonic Research*, 18(1), pp. 11-20; <https://doi.org/10.15251/JOR.2022.181.11>
- [31] Mulliken, R. S. (1955). Electronic population analysis on LCAO-MO molecular wave functions. I. *The Journal of Chemical Physics*, 23(10), 1833-1840; <https://doi.org/10.1063/1.1740588>
- [32] Segall, M. D., Shah, R., Pickard, C. J., & Payne, M. C. (1996). Population analysis of plane-wave electronic structure calculations of bulk materials. *Physical Review B*, 54(23), 16317; <https://doi.org/10.1103/PhysRevB.54.16317>